Meteoritics & Planetary Science 38, Nr 5, 767–781 (2003)
Abstract available online at http://meteoritics.org

Noble gases in ureilites released by crushing

Ryuji OKAZAKI,[1, 2†*] Tomoki NAKAMURA,[1] Nobuo TAKAOKA,[1] and Keisuke NAGAO[2]

[1]Department of Earth and Planetary Sciences, Faculty of Sciences, Kyushu University, Hakozaki, Fukuoka 812–8581, Japan
[2]Laboratory for Earthquake Chemistry, Graduate School of Science, University of Tokyo, Hongo, Bunkyo-ku, Tokyo 113–0033, Japan
[†]Present address: Department of Geological Sciences, Arizona State University, P. O. Box 871404, Tempe, Arizona 85287–1404, USA
[*]Corresponding author. E-mail: okazaki@asu.edu

(Received 3 June 2002; revision accepted 9 May 2003)

Abstract–Noble gases in two ureilites, Kenna and Allan Hills (ALH) 78019, were measured with two extraction methods: mechanical crushing in a vacuum and heating. Large amounts of noble gases were released by crushing, up to 26.5% of ^{132}Xe from ALH 78019 relative to the bulk concentration. Isotopic ratios of the crush-released Ne of ALH 78019 resemble those of the trapped Ne components determined for some ureilites or terrestrial atmosphere, while the crush-released He and Ne from Kenna are mostly cosmogenic. The crush-released Xe of ALH 78019 and Kenna is similar in isotopic composition to Q gas, which indicates that the crush-released noble gases are indigenous and not caused by contamination from terrestrial atmosphere. In contrast to the similarities in isotopic composition with the bulk samples, light elements in the crush-released noble gases are depleted relative to Xe and distinct from those of each bulk sample. This depletion is prominent especially in the ^{20}Ne/^{132}Xe ratio of ALH 78019 and the ^{36}Ar/^{132}Xe ratio of Kenna. The values of measured ^{3}He/^{21}Ne for the gases released by crushing are significantly higher than those for heating-released gases. This suggests that host phases of the crush-released gases might be carbonaceous because cosmogenic Ne is produced mainly from elements with a mass number larger than Ne.

Based on our optical microscopic observation, tabular-foliated graphite is the major carbon mineral in ALH 78019, while Kenna contains abundant polycrystalline graphite aggregates and diamonds along with minor foliated graphite. There are many inclusions at the edge and within the interior of olivine grains that are reduced by carbonaceous material. Gaps can be seen at the boundary between carbonaceous material and silicates. Considering these petrologic and noble gas features, we infer that possible host phases of crush-released noble gases are graphite, inclusions in reduction rims, and gaps between carbonaceous materials and silicates.

The elemental ratios of noble gases released by crushing can be explained by fractionation, assuming that the starting noble gas composition is the same as that of amorphous carbon in ALH 78019. The crush-released noble gases are the minor part of trapped noble gases in ureilites but could be an important clue to the thermal history of the ureilite parent body. Further investigation is needed to identify the host phases of the crush-released noble gases.

INTRODUCTION

Ureilites are achondritic meteorites, most of which consist predominantly of coarse-grained olivine and pigeonite (Vdovykin 1970; Goodrich 1992; Mittlefehldt et al. 1998). Most ureilites contain abundant carbon (up to 5.9 wt% for North Haig; Grady et al. 1985) comparable to carbonaceous (C) chondrites (5.8 wt% for the Tagish Lake C chondrite; Grady et al. 2002). Various degrees of impact shocks are also characteristic of ureilites. Graphite is the most common polymorph of carbonaceous material in ureilites. Diamonds have been identified in such shocked ureilites as Dyalpur (Mori and Takeda 1988), Goalpara (Vdovykin 1970; Göbel et al. 1978), Haverö (Marvin and Wood 1972), and Kenna (Gibson 1976; Berkley et al. 1976). One of the least shocked ureilites, Allan Hills 78019 (ALH 78019), contains no diamonds (Berkley and Jones 1982; Wacker 1986; Nakamuta and Aoki 2000; Nakamuta et al. 2002), while the less shocked ureilite, Dar al Gani (DaG) 868 (Takeda et al. 2001), was found to contain diamonds.

The origin of diamonds in ureilites is controversial because diamonds can be produced through a variety of mechanisms:

1. Transformation by impact shock (Lipschutz 1964;

Vdovykin 1970; Bischoff et al. 1999; Nakamura et al. 2000; Nakamuta and Aoki 2000, 2001; Nakamuta et al. 2002; Takeda et al. 2001).
2. Chemical vapor deposition (CVD) under low-pressure conditions (Derjaguin et al. 1968; Sato et al. 1984; Fukunaga et al. 1987; Matsuda et al. 1991, 1995).
3. Transformation under high static pressure (Urey 1956; Ringwood 1960; Carter and Kennedy 1964).

Catalytic transformation of graphite to diamonds (Nakamuta and Aoki 2001; Takeda et al. 2001) can explain the presence of diamonds in the weakly shocked ureilite DaG 868. Ureilites are unlikely to be from a parent body large enough to produce a sufficiently high pressure for diamonds to form (Anders and Lipschutz 1966; Vdovykin 1970). CVD is also unlikely for ureilite diamonds because petrographical features of graphite and diamonds in ureilites is not consistent (e.g., Takeda et al. 2001) with the CVD origin.

The origin of trapped (or primordial) noble gases in ureilites is also enigmatic (e.g., Göbel et al. 1978). Some ureilites contain trapped Ar, Kr, and Xe in abundances comparable to C chondrites (e.g., Mazor et al. 1970), although they show well-crystallized olivine and pyroxene textures and are depleted in the other volatile elements (e.g., Goodrich 1992). Carbonaceous material, diamonds, and amorphous carbon are known to be some of the main noble-gas carriers in ureilites (Weber et al. 1971, 1976; Wilkening and Marti 1976; Göbel et al. 1978; Wacker 1986; Rai et al. 2002). Thus, we expect that the origin of noble gases could be related to that of carbonaceous material.

Besides diamonds and amorphous carbon, the presence of at least one more trapping site of noble gases has been predicted, based on the differences in noble gas elemental ratios found in the bulk samples and carbonaceous materials (Mazor et al. 1970; Weber et al. 1971; Göbel et al. 1978). In these previous studies, carbonaceous materials were separated by pulverization and/or acid treatments. To study the influence of the sample pulverization, we measured noble gases extracted by mechanical crushing in a vacuum. Conventional pyrolyses were also performed to compare the bulk compositions with the compositions of the crush-released gases. The analyzed meteorites were Kenna and ALH 78019, which are different in shock degree and the mode of occurrences of carbon polymorphs. Kenna is a mildly shocked ureilite and contains both graphite and diamonds (Berkley et al. 1976), while ALH 78019 is the least shocked ureilite with abundant graphite and no diamonds (Berkley and Jones 1982; Wacker 1986; Nakamura et al. 2000; Nakamuta and Aoki 2000; Nakamuta et al. 2002).

SAMPLES AND EXPERIMENTAL METHODS

Noble gases were extracted by mechanical crushing in a vacuum and by heating (pyrolysis). The mechanical crushing enables us to preferentially release noble gases residing in fragile phases such as microbubbles, healed cracks within silicates, or grain boundaries. The samples for crushing analyses were sliced to about 800 μm in thickness (about 90 mg in weight) using a diamond blade. We have used the diamond blade for cutting other non-chondritic meteorites and have never observed any contamination of noble gases. The pestle used for the crushing is made of stainless steel (about 50 g) and operated by an electromagnet, while the crucible is made of Mo. Noble gases in each specimen were extracted by stepwise crushing to investigate variations in concentrations and isotopic and elemental ratios among crushing cycles. We continued crushing samples until the amounts of released gases were low and did not change significantly (see Fig. 5), and thus, we obtained the total amounts of gases residing in phases destructed and degassed by crushing for each meteorite. The step-crushing extractions were performed in 4 and 6 cycles, and each crushing cycle consists of 300–600 strokes. The total number of strokes was 1200 and 2400 for ALH 78019 and Kenna, respectively. After crushing and measuring the noble gases, the crushed samples (AC and KC) were collected from the Mo crucibles to investigate size distributions and morphology of the carbonaceous material. The abundances of each size fraction of the crushed samples are shown in Fig. 1. The particle diameter of the crushed Kenna sample (KC) is mostly <95 μm, while that of the ALH 78019 sample (AC) shows a bimodal distribution at 45–95 and <305 μm. The difference in

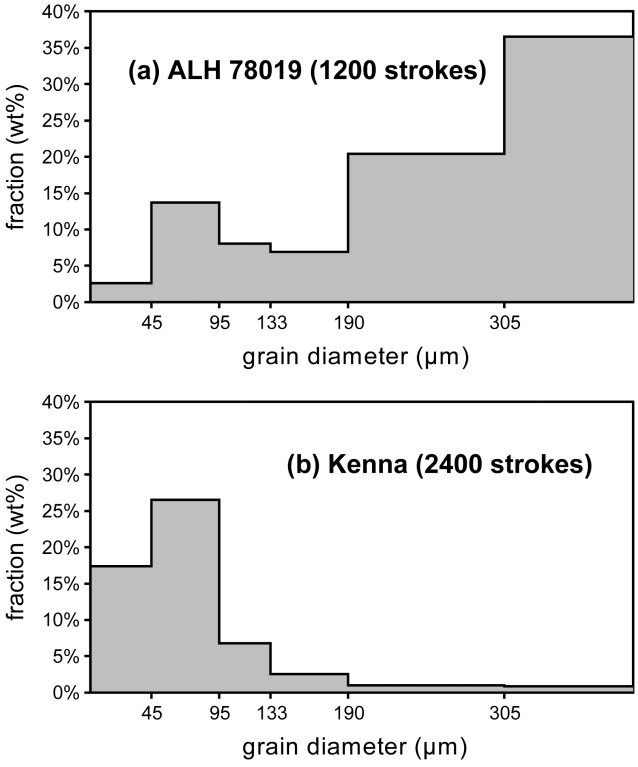

Fig. 1. Size distributions of ALH 78019 and Kenna samples after the crushing experiments.

the particle diameter of the crushed samples could be related to the fragility of these meteorites and/or the total number of crushing strokes. We investigated carbon-rich fractions separated from the fine-grained fractions (<95 μm) of each ureilite using a scanning electron microprobe (SEM) at the Kyushu University (Jeol JSM-5800LV). Some of the carbonaceous material in the coarse-grained fraction (>305 μm) from ALH 78019 is contained inside silicates, while the carbonaceous material in the fine-grained fraction (<95 μm) is broken and separated from silicates. Most of the post-crushing carbonaceous material in Kenna is fine-grained.

Noble gas measurements by pyrolysis were also performed for the crushed samples to compare the isotopic and elemental ratios with those of the crush-released gases. We prepared a sample of ALH 78019 (AP2 of 11.2 mg) from a fraction of the crushed sample with >305 μm diameter. The post-crushing sample of Kenna (KP2 of 6.9 mg) was from an aliquot (<95 μm diameter fraction) of the crushed sample. In addition to these samples, whole rock samples for pyrolysis analyses (AP1 of 9.3 mg and KP1 of 23.6 mg) were prepared from each ureilite. Each sample was heated stepwise at 600, 1800, and 1850°C to separately extract atmospheric gases adsorbed on the samples (600°C fractions) and to check complete degassing of the samples (1850°C fractions). Kr and Xe isotope ratios of the 1850°C steps were not measured, except for KP1, because Kr and Xe amounts in the 1850°C step were comparable to the blank. We adopt the summations of noble gases released at 600–1850°C as the "total" concentrations as shown in Table 2 and the Appendix.

Evolved noble gases were purified through our standard procedure described previously (e.g., Nagao et al. 1999), and were analyzed with a modified VG5400 mass spectrometer (MS-II) at the Laboratory for Earthquake Chemistry, University of Tokyo. Mass discrimination and sensitivities of the mass spectrometer were calibrated by measuring known amounts of atmospheric noble gases and helium standard gas ($^3He/^4He = 1.71 \times 10^{-4}$). Detection limits of the mass spectrometer using the ion-counting system (secondary electron multiplier SEV217, Balzers Corp.) are about 1×10^{-15} and 1×10^{-16} cm^3 STP for He-Ne and Ar-Xe, respectively. Blank levels for crushing (500 strokes) and pyrolysis (at 600 and 1850°C) are presented in the Appendix.

In Tables 1 and 2, measured noble gases are decomposed into trapped and cosmogenic components (the subscript "t" represents a trapped component, while "c" represents a cosmogenic component). In the calculation of $^{20}Ne_t$ and $^{36}Ar_t$ concentrations, we subtracted contributions of cosmogenic gases with the following assumptions: $(^{20}Ne/^{22}Ne)_t = 10.4$ (Ne-U; Ott et al. 1984); $(^{20}Ne/^{22}Ne)_c = 0.8574$ (KP2–1800 in the Appendix); $(^{38}Ar/^{36}Ar)_t = 0.18627$ (AP1–1800 in the Appendix); $(^{38}Ar/^{36}Ar)_c = 1.5$ (Ozima and Podosek 2002). The $^{38}Ar/^{36}Ar$ for AP1–1800 is lower than the usual planetary-gas value (0.188). Similar $^{38}Ar/^{36}Ar$ ratios were reported for other ureilites (e.g., Bogard et al. 1973; Göbel et al. 1978). Concentrations of $^{21}Ne_c$ are calculated using $(^{21}Ne/^{22}Ne)_t = 0.027$ (Ne-U; Ott et al. 1984) and $(^{21}Ne/^{22}Ne)_c = 0.8782$ (KP2-1800 in the Appendix).

We applied blank corrections for both crushing and pyrolysis. In most cases, the blank levels for $^{36, 38}$Ar, Kr, and Xe are lower than 1%, while those for ^{4}He and ^{40}Ar are >20% in some fractions (e.g., ^{4}He of AP and ^{40}Ar of KC). The amounts of ^{21}Ne released from AC are small and comparable to those of the blank ^{21}Ne emitted principally from the ion source of the mass spectrometer. Uncertainties for concentrations of the measured noble gases (Appendix) are estimated to be 10% based on uncertainties for sensitivities of the mass spectrometer (5%) and those for blank gas abundances (10%). We calculated 10–20% uncertainties for $^{20}Ne_t$ released by crushing Kenna (KC-1 to KC-6: Table 2) by propagation of uncertainties of measured $^{20}Ne/^{22}Ne$ and ^{20}Ne, where we neglected uncertainties for the assumed $(^{20}Ne/^{22}Ne)_t$ and $(^{20}Ne/^{22}Ne)_c$ ratios. The uncertainties for $^{21}Ne_c$ and $^{36}Ar_t$ were determined similarly as those for $^{20}Ne_t$.

RESULTS

Trapped Noble Gases Released by Crushing

Large amounts of heavy noble gases were released from ALH 78019 and Kenna by crushing. Cumulative releases by crushing relative to bulk concentrations (AC to AP1; KC to KP1) of measured ^{36}Ar, ^{84}Kr, and ^{132}Xe are as follows: 23, 27, and 27% after 1200 strokes for ALH 78019 and 5, 13, and 19% after 2400 strokes for Kenna, respectively. Fractions of crush-released He and Ne are smaller relative to ^{36}Ar, ^{84}Kr, and ^{132}Xe: measured ^{3}He, ^{4}He, ^{20}Ne, and ^{21}Ne are 1.7, 2.7, 6.5, and 0.35% for ALH 78019 and 1.3, 1.3, 0.64, and 0.48% for Kenna, respectively.

As shown in Fig. 2, crush-released Ne of ALH 78019 (AC) is isotopically similar to trapped Ne deduced from noble gases in carbonaceous materials separated from some ureilites ($^{20}Ne/^{22}Ne$ ranges from 10.4 to 10.8; Göbel et al. 1978; Ott et al. 1984; Wacker 1986). The $^{20}Ne/^{22}Ne$ ratios determined at 600°C for AP1 and AP2 are similar to those for AC (Appendix). If the Ne released by crushing and heating at 600ºC were atmospheric, the estimated contributions from the atmospheric ^{40}Ar on AC–1 and AP1–600 would be at least 1.97×10^{-7} and 1.45×10^{-7} cm^3 STP/g, respectively (assuming the non-fractionated atmospheric $^{20}Ne/^{40}Ar$, i.e., for the lower limit of ^{40}Ar contaminations). Notwithstanding, the estimated ^{40}Ar concentrations are larger than the measured ^{40}Ar for AC–1 and AP1–600 of 1.70×10^{-7} and 1.65×10^{-7} cm^3 STP/g, respectively. Thus, it is reasonable to think that the Ne released from ALH 78019 by crushing and heating at 600ºC is not dominantly from the terrestrial atmosphere but represents indigenous trapped gas. Unlike the 600ºC fractions, the 1800ºC fractions show evident contributions from

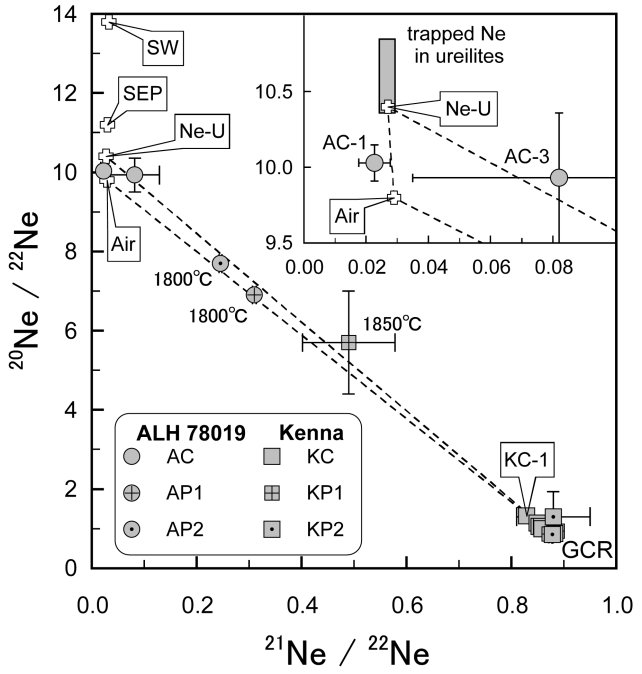

Fig. 2. A plot of Ne isotopes for ALH 78019 and Kenna. All data (except for KP1–1850) plot within an area representing mixing of cosmogenic Ne, terrestrial atmospheric Ne (Ozima and Podosek 2002), and Ne-U (Ott et al. 1984). The shaded area in the inset indicates the compositional range of trapped noble gases in ureilites (Göbel et al. 1978; Ott et al. 1984; Wacker 1986). The isotope ratios of Ne for solar wind (SW: Benkert et al. 1993) and solar energetic particles (SEPs: Benkert et al. 1993) are also plotted for comparison. Abbreviations: AC and KC, crushing data of ALH 78019 and Kenna, respectively; AP1/AP2 and KP1/KP2, pyrolysis data of ALH 78019 and Kenna, respectively.

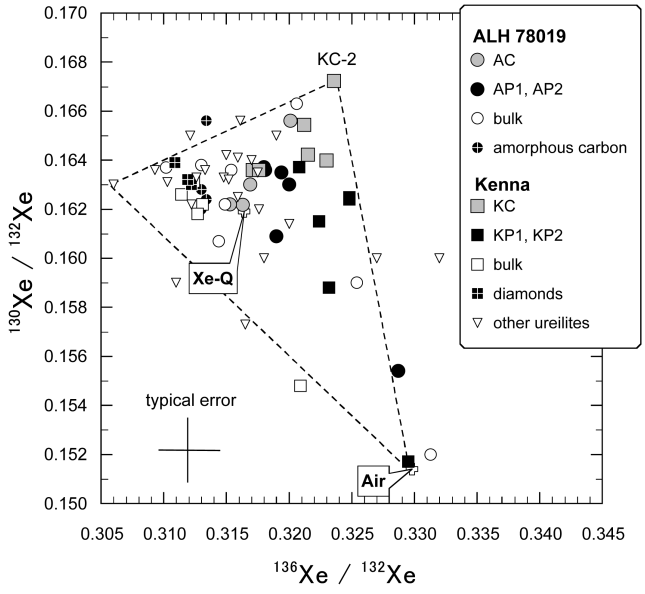

Fig. 3. Isotopic ratios of ^{130}Xe/^{132}Xe and ^{136}Xe/^{132}Xe for Kenna and ALH 78019. The isotopic ratios of crush-released Xe are similar to those of Xe determined for bulk samples, plotting around Xe-Q (Busemann et al. 2000). Data sources for bulk and C-rich separates of other ureilites: Marti (1967); Mazor et al. (1970); Weber et al. (1971, 1976); Bogard et al. (1973); Wilkening and Marti (1976); Wacker (1986); Goodrich et al. (1987). The abbreviations are the same as in Fig. 2.

cosmogenic Ne (Fig. 2), suggesting that the cosmogenic Ne is more tightly bound than the trapped Ne. Probably, cosmogenic noble gases are enclosed tightly in lattice defects of the host minerals and released at high temperatures. For the crushing measurements, the cosmogenic Ne is released only from the surface and cracks newly formed by crushing. The total ^{3}He/^{4}He determined by crushing for ALH 78019 (0.0061) is about half of that for AP1 (0.01105). This suggests that the crush-released He also contains a lower proportion of cosmogenic gases than the He released by heating, though we cannot rule out an enrichment of radiogenic ^{4}He in AC.

Krypton and Xe released by the crushing of both Kenna and ALH 78019 are similar in isotopic composition to those of the bulk samples of each ureilite (Fig. 3 and Appendix), although, Xe isotopes of some fractions are distinct from values reported previously (this will be discussed in the next section). Kr and Xe are mostly composed of trapped gases as indicated in the ^{78}Kr/^{84}Kr and ^{126}Xe/^{132}Xe ratios (Appendix), which are identical to those of "Q" or "P1" gas (e.g., Wieler et al. 1992; Huss et al. 1996; Busemann et al. 2000). This is consistent with the conclusion based on the crush-released Ne from ALH 78019.

In contrast to the similarities of the isotopic compositions of Kr and Xe with noble gases in bulk samples and carbonaceous materials (Wilkening and Marti 1976; Göbel et al. 1978; Ott et al. 1984; Wacker 1986), there are striking differences in the elemental ratios between crush-released noble gases and the bulk compositions (Table 1 and Fig. 4). The elemental ratios of the trapped noble gases ^{20}Ne$_t$/^{36}Ar$_t$/^{84}Kr/^{132}Xe for ALH 78019 determined by crushing are 1.24/353/1.93/1 against 5.84/413/2.04/1 for the bulk sample (Table 1). The ^{20}Ne$_t$/^{132}Xe ratio of crush-released gases from ALH 78019 (AC) is 5 times lower than that for the bulk sample (Table 1 and Fig. 4a), while the ^{36}Ar$_t$/^{132}Xe and ^{84}Kr/^{132}Xe ratios are similar to those of the bulk sample (Table 1 and Fig. 4b). The ^{20}Ne/^{132}Xe ratio for AC (1.24) is different from that of the amorphous carbon from ALH 78019 (5.9–7.5; Wacker 1986). The ^{20}Ne$_t$/^{36}Ar$_t$/^{84}Kr/^{132}Xe ratios for Kenna (KC) are 0.177/31.3/0.581/1, while those for the bulk sample determined by heating (KP1) are 0.299/114/0.84/1 (Table 1). The depletion in the lighter noble gases of the crush-released gases can be seen especially in the ^{36}Ar$_t$/^{132}Xe ratio of KC (Fig. 4b). Noble gases in diamonds from Kenna could be enriched in the light elements relative to the bulk composition, according to the results for the Haverö ureilite: the ^{36}Ar/^{132}Xe ratio for diamonds from Haverö is 532, higher than 400 determined for the bulk sample (Göbel et al. 1978). Therefore, the elemental ratios of the crush-released noble gases from Kenna are different from those of noble gases in the diamonds (Göbel et al. 1978; Wacker 1986).

Table 1. Elemental ratios of noble gases in ALH 78019 and Kenna.

	$^{20}Ne_t/^{132}Xe$	$^{36}Ar_t/^{132}Xe$	$^{84}Kr/^{132}Xe$	$^{3}He/^{21}Ne$[a]
ALH 78019				
Crushing AC (0.0871 g)				
AC–1 (300 strokes)	1.06 ± 0.16	377 ± 57	2.00 ± 0.30	18.8 ± 2.8
AC–2 (300 strokes)	1.40 ± 0.21	260 ± 39	1.75 ± 0.26	>12.4
AC–3 (300 strokes)	2.44 ± 0.37	343 ± 52	1.63 ± 0.24	>11.5
AC–4 (300 strokes)	2.22 ± 0.33	349 ± 52	1.88 ± 0.28	>12.0
Total	1.24 ± 0.19	353 ± 53	1.93 ± 0.29	18.8 ± 2.8
Pyrolysis AP1 (0.0093 g)				
AP1–600 (600ºC)	5.68 ± 0.86	250 ± 37	1.78 ± 0.27	(18.6)[b]
AP1–1800 (1800ºC)	5.09 ± 0.76	417 ± 63	2.06 ± 0.31	4.72 ± 0.71
AP1–1850 (1850ºC)	<10.9	308 ± 46	1.41 ± 0.21	(9.49)[b]
Total	5.11 ± 0.77	410 ± 61	1.99 ± 0.30	4.72 ± 0.71
Pyrolysis AP2 (0.0112 g)				
AP2–600 (600ºC)	3.04 ± 0.46	104 ± 16	1.60 ± 0.24	(21.7)[b]
AP2–1800 (1800ºC)	6.8 ± 1.0	438 ± 66	2.13 ± 0.32	5.34 ± 0.80
AP2–1850 (1850ºC)	<19.2	271 ± 41	1.29 ± 0.19	(11.0)[b]
Total	6.6 ± 1.0	416 ± 62	2.09 ± 0.31	5.34 ± 0.80
Kenna				
Crushing KC (0.0898 g)				
KC–1 (300 strokes)	0.260 ± 0.039	38.7 ± 5.8	0.657 ± 0.098	11.7 ± 1.8
KC–2 (300 strokes)	0.158 ± 0.024	28.5 ± 4.3	0.551 ± 0.083	10.0 ± 1.5
KC–3 (300 strokes)	0.120 ± 0.021	22.9 ± 3.4	0.518 ± 0.078	9.0 ± 1.4
KC–4 (300 strokes)	0.147 ± 0.033	29.5 ± 4.4	0.558 ± 0.084	8.9 ± 1.3
KC–5 (600 strokes)	0.173 ± 0.030	31.4 ± 4.7	0.576 ± 0.086	8.0 ± 1.2
KC–6 (600 strokes)	0.116 ± 0.026	33.2 ± 5.0	0.572 ± 0.086	9.5 ± 1.4
Total	0.177 ± 0.055	31.3 ± 4.7	0.581 ± 0.087	9.7 ± 1.5
Pyrolysis KP1 (0.0236 g)				
KP1–600 (600ºC)	1.19 ± 0.30	51.2 ± 7.7	1.91 ± 0.29	88 ± 13
KP1–1800 (1800ºC)	0.276 ± 0.059	115 ± 17	0.82 ± 0.12	2.80 ± 0.42
KP1–1850 (1850ºC)	7.9 ± 1.3	194 ± 29	1.22 ± 0.18	<13.7
Total	0.299 ± 0.090	114 ± 17	0.84 ± 0.13	3.72 ± 0.56
Pyrolysis KP2 (0.0069 g)				
KP2–600 (600ºC)	0.14 ± 0.13	14.9 ± 2.2	1.26 ± 0.19	80 ± 12
KP2–1800 (1800ºC)	= 0	208 ± 31	1.27 ± 0.19	2.12 ± 0.32
KP2–1850 (1850ºC)	<1.9	124 ± 19	0.94 ± 0.14	<2.72
Total	0.14 ± 0.13	171 ± 26	1.26 ± 0.19	3.89 ± 0.58

[a]Not corrected for contributions of trapped gases.
[b]Not corrected for contributions of the blank.

Unlike ALH 78019, isotopic ratios of the crush-released Ne of Kenna (KC) are almost cosmogenic, showing a slight shift toward trapped Ne composition (Fig. 2) at the first crushing step (KC–1). The $^{3}He/^{4}He$ ratio of the crush-released gases from Kenna is also close to the cosmogenic value of 0.2 (Ozima and Podosek 2002). Hence, He and Ne in Kenna are dominated by cosmogenic gases, which is consistent with the long cosmic ray exposure age of 23 Ma (Wilkening and Marti 1976) as compared to that for ALH 78019 (~0.1 Ma; Wacker 1986). Note that measured $^{3}He/^{21}Ne$ ratios of the crush-released gases (~20 and 10 for AC and KC, respectively) are higher than those of the pyrolysis-released gases (~5 and 4 for AP1 and KP1, respectively). The correlation between the $^{3}He/^{21}Ne$ and $^{22}Ne/^{21}Ne$ ratios for KP1 is in good agreement with that for bulk chondrites (Eberhardt et al. 1966; Nishiizumi et al. 1980). Thus, the high $^{3}He/^{21}Ne$ ratio of KC compared to that of KP1 must be due to cosmogenic ^{3}He emitted from phases in which the production rate of cosmogenic ^{3}He is higher than in the whole rock. Preferential release of ^{3}He by crushing is not responsible for the high $^{3}He/^{21}Ne$ ratio because the cosmogenic $^{21}Ne/^{38}Ar$ ratio for KC (~5) is lower than that for KP1 (~13), which probably reflects the large contribution on the crush-released Ar from $^{38}Ar_c$ in sulfides and/or metal phases. The variation within crushing cycles for each meteorite may reflect the existence of more than one phase having different noble gas compositions. Therefore, the

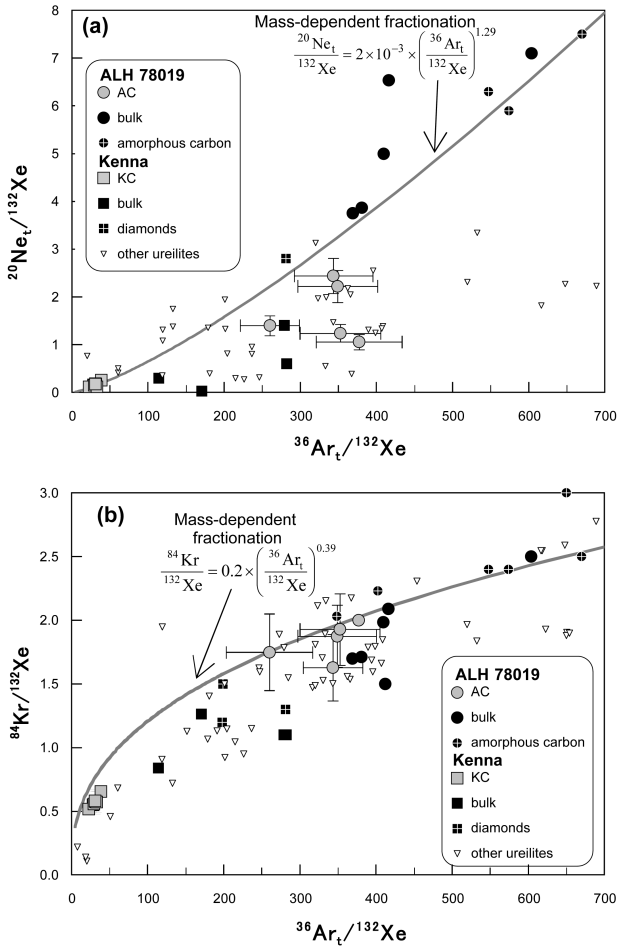

Fig. 4. Elemental ratios of the trapped noble gases in ALH 78019 and Kenna. Crush-released noble gases of ALH 78019 and Kenna are depleted in trapped ^{20}Ne (a) and ^{36}Ar (b) compared with those in each bulk sample, respectively. The dotted lines show theoretical curves of fractionations by diffusive migration (Aston 1933). The calculation method of the theoretical lines is mentioned in the text in detail. Data sources: Müller and Zähringer (1969); Mazor et al. (1970); Weber et al. (1971, 1976); Bogard et al. (1973); Wilkening and Marti (1976); Göbel et al. (1978); Ott et al. (1984, 1985, 1986, 1993); Wacker (1986); Goodrich et al. (1987); Rai et al. (2001, 2002); Takaoka et al. (2001).

unidentified host phases of the crush-released noble gases (at least for the cosmogenic component) consist mainly of elements lighter than Ne because cosmogenic Ne is produced mainly from target nuclides with larger mass numbers than Ne. Carbon is the most plausible element for such target nuclides. Oxygen would also work, but it is usually associated with heavier elements, as found in silicates. We will discuss the possible candidates for the unidentified host phases of the crush-released noble gases in a later section. The measured ^{3}He/^{21}Ne ratios of AC (~20) are higher than those of KC (~10; Table 1). This might result from differences in the abundance ratio of carbonaceous materials compared to other minerals (silicates, sulfides, and metals) as the host phases of crush-released gases.

Based on a comparison of ALH 78109 with Kenna, we obtained information on the host phases of the crush-released gases. Fig. 5 shows the amounts of gases released by crushing at each step against the number of crushing strokes. The vertical axis shows the cumulative amounts of crush-released noble gases. For ALH 78019, 60–80% of gases were released at the first crushing cycle, and the fraction steeply decreases to 10–30% at the second cycle (Fig. 5). The fractions of crush-released gases of Kenna are 30–40% and 20–25% for the first and second cycles, respectively. This implies that the carrier phases of the crush-released noble gases in Kenna are more resistant against crushing than those in ALH 78019.

The total remaining concentrations of the noble gases that were released at 600–1850°C from the coarse-grained (>305 μm in diameter) sample of ALH 78019 after crushing (AP2) are essentially identical to those of the whole rock sample (AP1). This might reflect the survival of the noble-gas host phases, as AP2 consists mainly of coarse silicate grains that were picked up from the post-crushing sample and that contain carbonaceous material within the silicates (Samples and Experimental Methods section). Concentrations of Ar, Kr, and Xe are lower in the post-crushing sample of Kenna with a <95 μm diameter (KP2) than those in the uncrushed whole rock sample (KP1), although, the He and Ne concentrations agree with each other. The disagreement in the heavy noble gas concentrations could be because heavy noble gases were released by crushing from the fine-grained fraction or because heavy noble gases survived in the coarse-grained fractions (>95 μm).

Heterogeneities in Compositions and Distributions of Noble Gases in Ureilites

The isotopic ratios of the Xe of ALH 78019 and Kenna are shown in Fig. 3 along with other ureilite data (Marti 1967; Mazor et al. 1970; Weber et al. 1971, 1976; Bogard et al. 1973; Wilkening and Marti 1976; Wacker 1986; Goodrich et al. 1987). The crush-released Xe of ALH 78019 and Kenna show excesses in isotopes except for ^{129}Xe, ^{131}Xe, and ^{132}Xe as compared to Xe of the carbon-rich acid residues (Wacker 1986). The excesses observed in AC and KC cannot be explained by contamination from atmospheric gases (unlike the 600ºC fractions) or mass fractionation effects in the laboratory. The variable Xe isotopes in ureilites suggest that the trapped Xe in ureilites consist of at least one more component aside from those residing in diamonds (Weber et al. 1971, 1976; Göbel et al. 1978; Wilkening and Marti 1976) and amorphous carbon (Wacker 1986; Rai et al. 2002). Although mixing of Xe-Q, Xe-S (in presolar SiC; Lewis et al. 1994), and Xe-HL (in presolar diamond; Huss and Lewis 1994a, 1994b) could produce a Xe spectrum similar to those for AC and KC, the Xe-S and Xe-HL components are accompanied by Ne-E(H) (Huss and Lewis 1995) and Ne-HL (Huss and Lewis 1994b), respectively. These components

Table 2. Concentrations of trapped noble gases of ALH 78019 and Kenna.[a]

	$^{20}Ne_t$[b]	$^{36}Ar_t$[b]	^{84}Kr	^{132}Xe	$^{21}Ne_c$[c]
ALH 78019					
Crushing AC (0.0871 g)					
AC–1 (300 strokes)	0.345 ± 0.035	123 ± 12	0.652 ± 0.065	0.326 ± 0.033	<0.00131
AC–2 (300 strokes)	0.117 ± 0.012	21.7 ± 2.2	0.146 ± 0.015	0.0835 ± 0.0084	<0.000645
AC–3 (300 strokes)	0.0618 ± 0.0062	8.69 ± 0.87	0.0412 ± 0.0041	0.0253 ± 0.0025	<0.000323
AC–4 (300 strokes)	0.0373 ± 0.0038	5.86 ± 0.59	0.0315 ± 0.0032	0.0168 ± 0.0017	<0.00025
Total	0.56 ± 0.11	159 ± 32	0.87 ± 0.17	0.452 ± 0.090	<0.00253
(AC after 1200 strokes) AP1	6.8% ± 1.7%	23.5% ± 6.2%	26.5% ± 7.0%	27.2% ± 7.2%	<0.71%
Pyrolysis AP1 (0.0093 g)					
AP1–600 (600ºC)	0.289 ± 0.029	12.7 ± 1.3	0.0907 ± 0.0091	0.0509 ± 0.0051	<0.0125
AP1–1800 (1800ºC)	7.99 ± 0.80	655 ± 66	3.23 ± 0.32	1.57 ± 0.16	0.354 ± 0.035
AP1–1850 (1850ºC)	<0.397	11.2 ± 1.1	0.0514 ± 0.0051	0.0364 ± 0.0036	<0.00778
Total	8.3 ± 1.2	679 ± 118	3.29 ± 0.57	1.66 ± 0.29	0.354 ± 0.035
Pyrolysis AP2 (0.0112 g)					
AP2–600 (600ºC)	0.340 ± 0.034	11.7 ± 1.2	0.179 ± 0.018	0.112 ± 0.011	<0.00972
AP2–1800 (1800ºC)	12.1 ± 1.2	775 ± 77	3.77 ± 0.38	1.77 ± 0.18	0.367 ± 0.037
AP2–1850 (1850ºC)	<0.431	6.06 ± 0.61	0.0288 ± 0.0029	0.0224 ± 0.0022	<0.00349
Total	12.4 ± 1.8	793 ± 137	3.98 ± 0.69	1.9 ± 0.33	0.367 ± 0.037
Kenna					
Crushing KC (0.0898 g)					
KC–1 (300 strokes)	0.112 ± 0.011	16.7 ± 1.7	0.283 ± 0.028	0.431 ± 0.043	0.180 ± 0.018
KC–2 (300 strokes)	0.0615 ± 0.006	11.1 ± 1.1	0.215 ± 0.022	0.390 ± 0.039	0.171 ± 0.017
KC–3 (300 strokes)	0.0298 ± 0.0037	5.69 ± 0.57	0.129 ± 0.013	0.249 ± 0.025	0.115 ± 0.012
KC–4 (300 strokes)	0.0211 ± 0.0035	4.25 ± 0.43	0.0803 ± 0.0080	0.144 ± 0.014	0.0920 ± 0.0092
Subtotal (KC–1 ~KC–4)	0.224 ± 0.056	37.7 ± 7.5	0.707 ± 0.071	1.21 ± 0.12	0.56 ± 0.11
(KC after 1200 strokes) KP1	9.2% ± 3.4%	4.0% ± 1.1%	10.3% ± 2.1%	14.8% ± 3.0%	0.343% ± 0.091%
KC–5 (600 strokes)	0.0343 ± 0.0040	6.22 ± 0.62	0.114 ± 0.011	0.198 ± 0.020	0.136 ± 0.014
KC–6 (600 strokes)	0.0164 ± 0.0023	4.68 ± 0.47	0.0806 ± 0.0081	0.141 ± 0.014	0.0927 ± 0.0093
Total	0.275 ± 0.086	49 ± 12	0.902 ± 0.090	1.55 ± 0.16	0.787 ± 0.19
(KC after 2400 strokes) KP1	11.2% ± 4.6%	5.2% ± 1.6%	13.1% ± 2.6%	18.9% ± 3.8%	0.48% ± 0.15%
Pyrolysis KP1 (0.0236 g)					
KP1–600 (600ºC)	0.166 ± 0.027	7.12 ± 0.71	0.265 ± 0.027	0.139 ± 0.014	1.76 ± 0.18
KP1–1800 (1800ºC)	2.22 ± 0.40	926 ± 93	6.60 ± 0.66	8.05 ± 0.81	161 ± 16
KP1–1850 (1850ºC)	0.0636 ± 0.0069	1.57 ± 0.16	0.00992 ± 0.0010	0.0081 ± 0.00081	0.0058 ± 0.0006
Total	2.45 ± 0.66	935 ± 162	6.9 ± 1.2	8.20 ± 1.4	163 ± 28
Pyrolysis KP2 (0.0069 g)					
KP2–600 (600ºC)	0.093 ± 0.054	10.2 ± 1.0	0.863 ± 0.086	0.686 ± 0.069	3.14 ± 0.31
KP2–1800 (1800ºC)	= 0	627 ± 63	3.84 ± 0.38	3.02 ± 0.30	135 ± 14
KP2–1850 (1850ºC)	<0.145	9.38 ± 0.94	0.0715 ± 0.0072	0.0759 ± 0.0076	0.0950 ± 0.0095
Total	0.093 ± 0.054	647 ± 112	4.77 ± 0.83	3.78 ± 0.66	138 ± 24

[a]Unit is 10^{-9} cm^3 STP/g.
[b]Corrected for contributions of cosmogenic gases.
[c]Corrected for contributions of trapped gases.

also affect the Ne isotopic ratios largely. Thus, the addition of these minor Xe components is unlikely. The KC–2 fraction shows the largest deviation from the Xe-Q (Fig. 3), and the deviation is 2–4%, which is larger than the experimental errors for each isotope (0.2–1%; Appendix). We need further data on ureilite noble gases through crushing experiments to discuss the origin of the excess Xe isotopes.

The concentrations and elemental ratios of the trapped ^{36}Ar, ^{84}Kr, and ^{132}Xe in the bulk samples of ALH 78019 and Kenna (AP1 and KP1) are different from the values reported previously (Wacker 1986; Rai et al. 2002; Wilkening and Marti 1976). Similar variations have also been observed for other ureilites (e.g., Mazor et al. 1970; Göbel et al. 1978; Ott et al. 1985). The variations in heavy noble gas compositions

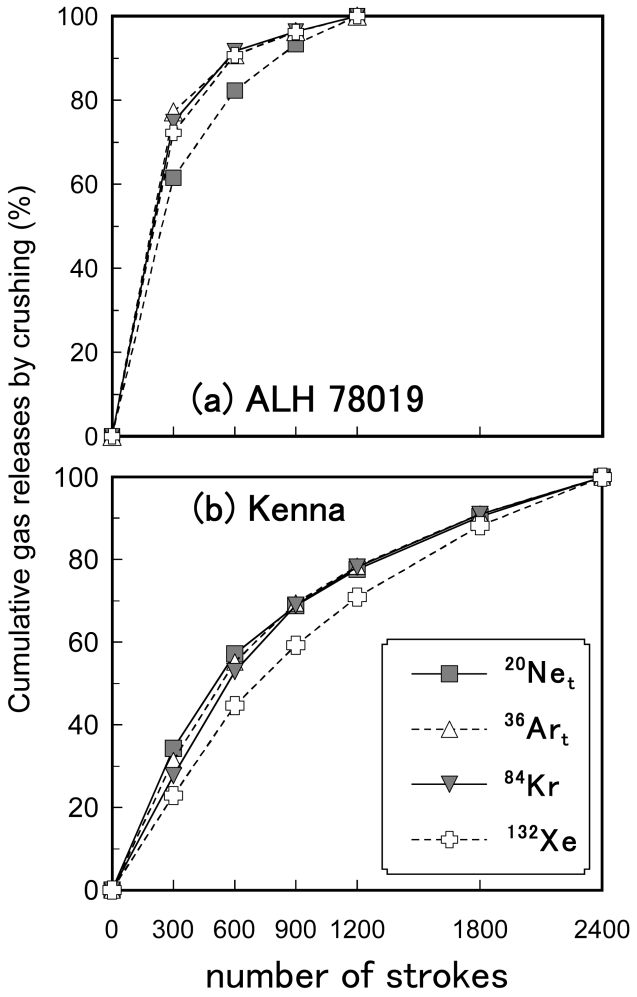

Fig. 5. Release patterns of the trapped noble gases during the crushing extraction. The vertical axis indicates cumulative releases of the crush-released noble gases.

could reflect a heterogeneous distribution on the cm scale (Ott et al. 1985) of the carrier phases and compositional differences of the trapped noble gas components.

DISCUSSION

Possible Trapping Phases of Crush-Released Noble Gases

Reportedly, in addition to diamond, at least one more carrier containing noble gases depleted in light elements exists, based on the differences in elemental ratios between the bulk sample and the diamond-rich separates of the Haverö ureilite (Göbel et al. 1978). A crushing experiment for the ureilite Yamato-791538 also showed that crush-released gases are depleted in Ar and Kr relative to Xe, as compared to noble gases in the bulk sample (Takaoka et al. 2001). Therefore, we can reasonably assume that ureilites generally contain fractionated noble gases in some fragile phases. Still, the fractionated noble gases could have variations in elemental compositions and concentrations for each ureilite. In this section, we will enumerate some possibilities for the host phases based on the noble gas and petrographical features of ALH 78019 and Kenna, although, drawing conclusions is difficult because only insufficient, circumstantial evidence exists.

Göbel et al. (1978) proposed that possible phases of the unidentified carriers are kamacite, chromite, and magnetite, based on the X-ray diffraction lines of the separated samples. Nonetheless, the chemical composition of these minerals cannot explain the high $^{3}He/^{21}Ne$ ratio of crush-released gas relative to those of the bulk samples (see section on Trapped Noble Gases Released by Crushing), though, no evidence exists that the fractionated noble gases in Haverö have a high $^{3}He/^{21}Ne$ ratio. The minerals reported in ureilites are olivine, pyroxene, kamacite, troilite, chromite, nickel-chrome, graphite, diamond, secondary (probably weathering-produced) oxides, and organic matters (Vdovykin 1970). The presence of amorphous carbon in ALH 78019 has also been suggested by Wacker (1986) and Rai et al. (2002). If trapped and cosmogenic gases that are simultaneously released by crushing are contained in a common phase, the unidentified host phase must be graphite, diamond, amorphous carbon, and/or organic matter; i.e., a phase that is composed only of carbon, hydrogen, and/or nitrogen. Otherwise, cosmogenic gases could originate from these materials while the trapped gases are released from gaps or inclusions.

Our optical microscopic observations have revealed that most graphite grains in ALH 78019 are well-crystallized and occur around and within olivine grains as blade-like shapes (Figs. 6a–6b; Nakamuta and Aoki 2000). The crystalline graphite in ALH 78019 is tabular-foliated and fragile, resembling micas (Fig. 6b). Kenna contains granular diamonds and polycrystalline graphite as the major carbon polymorphs (Fig. 6c), with minor foliated crystalline graphite. A common carbon polymorph to ALH 78019 and Kenna is graphite, though, the graphite fabric is different for each ureilite. We could not identify organic matter in either Kenna or ALH 78019. Post-crushing graphite in ALH 78019 was twisted (Fig. 6d) and could easily release noble gases during crushing. The polycrystalline graphite in Kenna was broken into small (10–20 μm) pieces by crushing. The interstices of the polycrystalline graphite layers might also be trapping sites. If trapped and cosmogenic gases are released from a common phase by crushing, graphite might be one possible candidate for the host phases of the crush-released noble gases. Neither diamonds nor amorphous carbon are plausible phases because their elemental ratios are different from those for the crush-released noble gases (Göbel et al. 1978; Wacker 1986; Rai et al. 2002), as mentioned above. While graphite in ureilites was reported to be free of noble gases (e.g., Weber et al. 1976; Göbel et al. 1978; Rai et al. 2002), pulverization during sample preparations might have released noble gases trapped weakly in graphite. The morphological difference between graphites contained in ALH 78019 and those in Kenna might

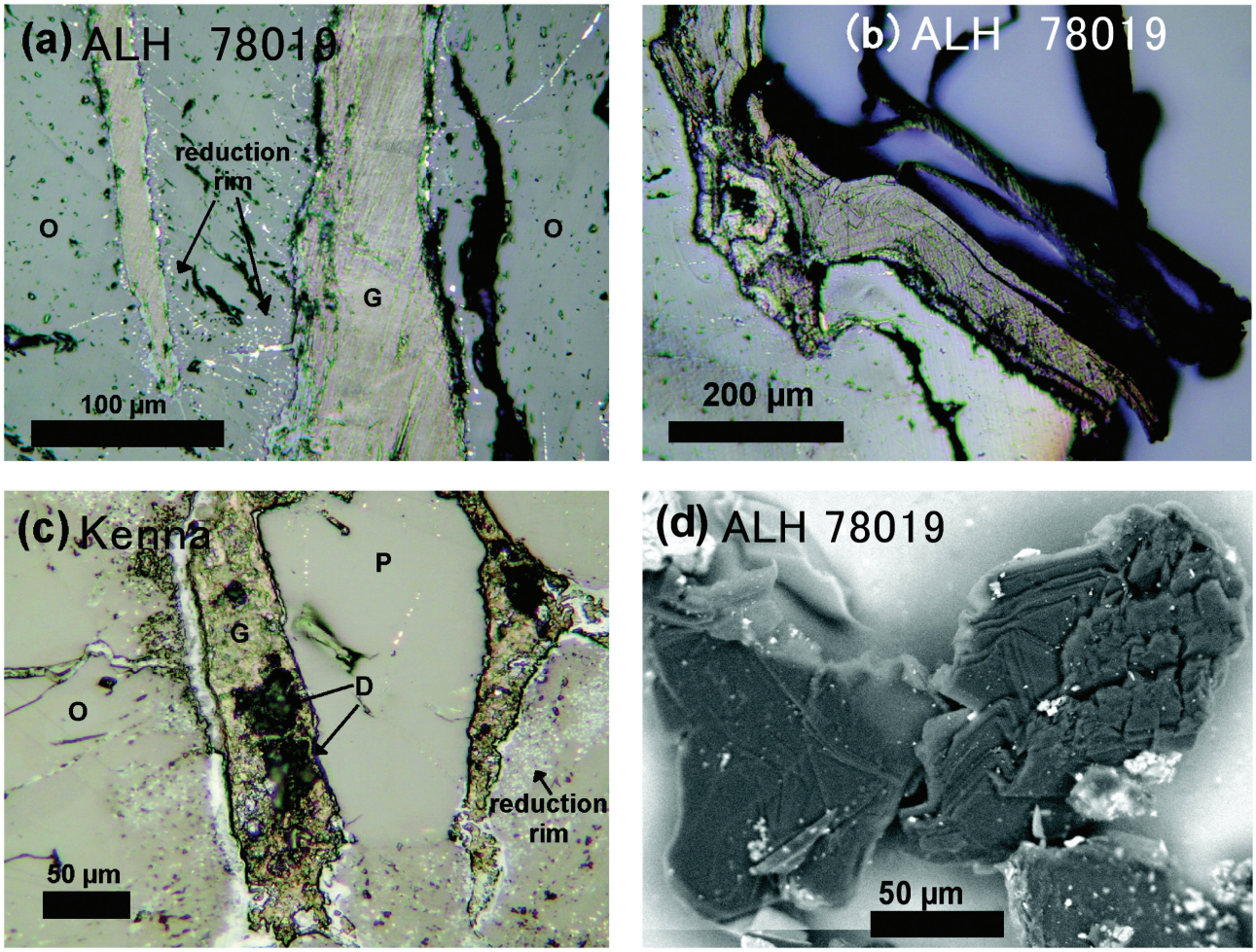

Fig. 6. Photomicrographs of carbonaceous phases (a–c: reflected light, d: back scattered electron image); a) graphite (G) in ALH 78019 is well crystallized and found within olivine crystals (O). Narrow reduction rims including small metal grains (light colored) grow in olivine grains contacted with carbonaceous material; b) the tabular-foliated graphite in ALH 78019; c) granular polycrystalline graphite in Kenna occurs preferentially in boundaries of olivine grains along with diamond clusters (D). Broad reduction rims can be seen in olivine but scarcely seen in pyroxene (P); d) Foliated graphite in ALH 78019 after crushing.

result in different release patterns (Fig. 5): polycrystalline graphite prominent in Kenna might be more retentive compared to foliated graphite in ALH 78019 because of their size difference. According to a study on ureilite noble gases by laser ablation (Nakamura et al. 2000), graphite in ALH 78019 contains trapped noble gases showing a $^{36}Ar/^{132}Xe$ ratio of 350–500, which supports our view about the carrier of the crush-released noble gases. We must determine the $^{20}Ne/^{132}Xe$ ratio of ALH 78019 graphite or the $^{36}Ar/^{132}Xe$ ratio of Kenna graphite because we cannot conclude whether noble gases in graphite released by laser ablation are the same as those released by crushing based on the $^{36}Ar/^{132}Xe$ ratio of ALH 78019 (Table 1 and Fig. 4).

Other possible trapping phases for trapped noble gases released by crushing are grain boundaries and/or inclusions. Under an optical microscope, finding inclusions in olivine grains is easy. Some portions, both of the edge and of the interior, of olivine grains adjacent to graphite in Kenna and ALH 78019 are reduced (Berkley et al. 1976; Berkley and Jones 1982) and contain numerous tiny metal blebs (the light color in Figs. 6a and 6c) in reduction rims. The reduction rims are thought to form as a result of reactions between olivine and carbon (Berkley et al. 1976; Wasson et al. 1976). We infer that reduction rims and gaps between olivine and carbonaceous materials might retain a part of the reaction products, such as gaseous carbon oxides and noble gases trapped originally in the carbonaceous material. The reduction rims are more prominent in Kenna than in ALH 78019 (Figs. 6a and 6c): Reduction rims in Kenna are 50–100 µm in width, while those in ALH 78019 are infrequent and typically smaller than 30 µm. Our crushing apparatus allows gentle crushing, and the sizes of crushed grains seem to converge at about 45–95 µm (Fig. 1). The steep decrease in the concentrations of the crush-released gases (Fig. 5) implies that most of the reduction rims in ALH 78019 were broken at the first crushing cycle, and only the minor parts released

noble gases in the subsequent cycles. For Kenna, ubiquitous reduction rims might liberate noble gases gradually during the crush sequence.

To identify the carrier phases of the crush-released gases, further noble gas measurements must be performed on graphite, organic matter, reduction rims, and the gaps between olivine and carbon phases with laser ablation or other methods.

Fractionation Effects on the Elemental Ratios of Crush-Released Noble Gases: Preferential Releases of Light Noble Gases

The elemental ratios of the noble gases released by crushing imply that the crush-released noble gases are fractionated by partial loss of light elements. The fractionation could not occur during crushing, as discussed above. Here, we show that the elemental ratios of the crush-released noble gases can be accounted for by fractionation during diffusive migration. We assume that amorphous carbon in ALH 78019 preserves the initial noble gas composition ($^{20}Ne/^{36}Ar/^{84}Kr/^{132}Xe$ = 7.49/668/2.53/1; Wacker 1986) and that some heating events in the parent body cause the migration of the noble gases into the unidentified phases that release the gases by crushing. Cosmogenic gases were produced after the heating processes and the ejection from the parent body, and thus they are not affected by the fractionation. Based on these assumptions, we have evaluated the mass-dependent fractionation effects on the residual gases according to an equation of diffusive migration (Aston 1933).

$$R_f/R_i = (V_i/V_f)^{\frac{m_2 - m_1}{m_2 + m_1}} \quad (1)$$

where R and V mean elemental ratios and volumes of gases at initial i and final f conditions, respectively. m_1 and m_2 are mass numbers of relevant isotopes ($m_1 < m_2$).

As shown in Fig. 4, the theoretical curve for $^{36}Ar/^{84}Kr/^{132}Xe$ is in good agreement with data sets obtained by crushing and pyrolysis in this study and with those for bulk samples and carbonaceous material of other ureilites (Müller and Zähringer 1969; Mazor et al. 1970; Weber et al. 1971, 1976; Bogard et al. 1973; Wilkening and Marti 1976; Göbel et al. 1978; Ott et al. 1984, 1985; Wacker 1986; Goodrich et al. 1987; Rai et al. 2001, 2002; Takaoka et al. 2001). The deviations of the data points from the theoretical curve for the $^{20}Ne/^{36}Ar/^{132}Xe$ ratio (Fig. 4a) might suggest variations, especially in the $^{20}Ne/^{132}Xe$ ratio, in primordial noble gas compositions of ureilites because the data points in Fig. 4 do not fall on a single line.

If the trapping phases of the fractionated noble gases are identified, we can estimate the heating temperature and the duration of heating using the appropriate diffusion rates and the elemental ratios of noble gases. Mineralogical and petrological studies on the host phases could be clues to the conditions of the parent body processes, such as pressure and temperature. These pieces of information could help specify the heat source (e.g., shock heating or metamorphism) resulting in the noble gas fractionation and assist us in the understanding of the evolutional history of the ureilite parent body.

CONCLUSION

Large amounts of trapped noble gases in two ureilites, ALH 78019 and Kenna, were released by mechanical crushing in a vacuum. The cumulative releases by crushing relative to bulk concentrations of trapped ^{36}Ar, ^{84}Kr, and ^{132}Xe are as follows: 23.5, 26.5, and 27.2% after 1200 strokes for ALH 78019 and 5.2, 13.1, and 18.9% after 2400 strokes for Kenna, respectively. The isotopic ratios of Ne from ALH 78019 indicate that the noble gases released by crushing represent, largely, a trapped component. The isotopic ratios of Kr and Xe are similar to those of Q gas, supporting the conclusion from the Ne isotopes.

The crush-released noble gases were enriched in Xe as compared to noble gases in bulk samples, amorphous carbon (Wacker 1986; Rai et al. 2002), and diamonds (Göbel et al. 1978; Wacker 1986). Measured $^{3}He/^{21}Ne$ ratios determined in the gas released by crushing are higher than those for pyrolysis. ALH 78019 released the major part of the noble gases at the first crushing cycle, while amounts of the crush-released noble gases of Kenna gradually decreased with progressive crushing (Fig. 5). This suggests that the carrier phases of fractionated noble gases in Kenna are more resistant to mechanical crushing than those in ALH 78019.

The possible host phases of the noble gases released by crushing are graphite, reduction rims, and gaps between silicates and carbonaceous materials. At the present time, we cannot give convincing evidence for the trapping phases of the crush-released noble gases. To elucidate the thermal history of the ureilite parent body, we must identify the host phases of the crush-released noble gases.

Acknowledgments–We thank the National Institute of Polar Research for providing the sample of ALH 78019. We also thank H. Busemann, R. Wieler, and an anonymous reviewer for their critical comments and helpful reviews. This work was partly supported by the JSPS Research Fellowships for Young Scientists for R. Okazaki.

Editorial Handling—Dr. Rainer Wieler

REFERENCES

Anders E. and Lipschutz M. E. 1966. Critique of paper by N. L. Carter and G. C. Kennedy, “Origin of diamonds in the Canyon Diablo and Novo Urei meteorites.” *Journal of Geophysical Resarch* 71:643–661.

Aston F. W. 1933. *Mass spectra and isotopes.* London: Hodder Arnold. 248 p.

Benkert J. P., Baur H., Signer P., and Wieler R. 1993. He, Ne, and Ar from the solar wind and solar energetic particles in lunar ilmenites and pyroxenes. *Journal of Geophysical Research* 98: 13147–13162.

Berkley J. L. and Jones J. H. 1982. Primary igneous carbon in ureilites: Petrological implications. Proceedings, 13th Lunar and Planetary Science Conference. *Journal of Geophysical Research* 87:A353–A364.

Berkley J. L., Brown H. G. IV, Keil K., Carter N. L., Mercier J. C. C., and Huss G. 1976. The Kenna ureilite: An ultramafic rock with evidence for igneous, metamorphic, and shock origin. *Geochimica et Cosmochimica Acta* 40:1429–1437.

Bischoff A., Goodrich C. A., and Grund T. 1999. Shock-induced origin of diamonds in ureilites (abstract #1100). 30th Lunar and Planetary Science Conference. CD-ROM.

Bogard D. D., Gibson E. K., Jr., Moore D. R., Turner N. L., and Wilkin R. B. 1973. Noble gas and carbon abundances of the Haverö, Dingo Pup Donga, and North Haig ureilites. *Geochimica et Cosmochimica Acta* 37:547–557.

Busemann H., Baur H., and Wieler R. 2000. Primordial noble gases in "phase Q" in carbonaceous and ordinary chondrites studied by closed-system stepped etching. *Meteoritics & Planetary Science* 35:949–973.

Carter N. L. and Kennedy G. C. 1964. Origin of diamonds in the Canyon Diablo and Novo Urei meteorites. *Journal of Geophysical Research* 69:2403–2421.

Derjaguin B. V., Fedoseev D. V., Lukyanovich V. M., Spitzin B. V., Ryabov V. A., and Lavrentyev A. V. 1968. Filamentary diamond crystals. *Journal of Crystal Growth* 2:380–384.

Eberhardt P., Eugster O., Geiss J., and Marti K. 1966. Rare gas measurements in 30 stone meteorites. *Zeitschrift Naturforschung* 21a:414–426.

Fukunaga K., Matsuda J., Nagao K., Miyamoto M., and Ito K. 1987. Noble-gas enrichment in vapour-growth diamonds and the origin of diamonds in ureilites. *Nature* 328:141–143.

Gibson E. K. Jr. 1976. Nature of the carbon and sulfur phases and inorganic gases in the Kenna ureilite. *Geochimica et Cosmochimica Acta* 40:1459–1464.

Göbel R., Ott U., and Begemann F. 1978. On trapped noble gases in ureilites. *Journal of Geophysical Research* 83:855–867.

Goodrich C. A. 1992. Ureilites: A critical review. *Meteoritics* 27: 327–352.

Goodrich C. A., Keil K., Berkley J. L., Laul J. C., Smith M. R., Wacker J. F., Clayton R. N., and Mayeda T. K. 1987. Roosevelt County 027: A low-shock ureilite with interstitial silicates and high noble gas concentrations. *Meteoritics* 22: 191–218.

Grady M. M., Wright I. P., Swart P. K., and Pillinger C. T. 1985. The carbon and nitrogen isotopic composition of ureilites: Implications for their genesis. *Geochimica et Cosmochimica Acta* 49:903–915.

Grady M. M., Verchovsky A. B., Franchi I. A., Wright I. P., and Pillinger C. T. 2002. Light element geochemistry of the Tagish Lake CI2 chondrite: Comparison with CI1 and CM2 meteorites. *Meteoritics & Planetary Science* 37:713–735.

Huss G. R. and Lewis R. S. 1994a. Noble gases in presolar diamonds I: Three distinct components and their implications for diamond origins. *Meteoritics* 29:791–810.

Huss G. R. and Lewis R. S. 1994b. Noble gases in presolar diamonds II: Component abundances reflect thermal processing. *Meteoritics* 29:811–829.

Huss G. R. and Lewis R. S. 1995. Presolar diamond, SiC, and graphite in primitive chondrites: Abundances as a function of meteorite class and petrologic type. *Geochimica et Cosmochimica Acta* 59: 115–160.

Huss, G. R., Lewis R. S., and Hemkin S. 1996. The "normal planetary" noble gas component in primitive chondrites: Compositions, carrier, and metamorphic history. *Geochimica et Cosmochimica Acta* 60:3311–3340.

Lewis R. S., Amari S., and Anders E. 1994. Interstellar grains in meteorites: II. SiC and its noble gases. *Geochimica et Cosmochimica Acta* 58:471–494.

Lipschutz M. E. 1964. Origin of diamonds in the ureilites. *Science* 143:1431–1434.

Marti K. 1967. Isotopic composition of trapped krypton and xenon in chondrites. *Earth and Planetary Science Letters* 3:243–248.

Marvin U. B. and Wood J. A. 1972. The Haverö ureilite: Petrographic notes. *Meteoritics* 7:601–610.

Matsuda J., Fukunaga K., and Ito K. 1991. Noble gas studies in vapor-growth diamonds: Comparison with shock-produced diamonds and the origin of diamonds in ureilites. *Geochimica et Cosmochimica Acta* 55:2011–2023.

Matsuda J., Kusumi A., Yajima H., and Syono Y. 1995. Noble gas studies in diamonds synthesized by shock loading in the laboratory and their implications on the origin of diamonds in ureilites. *Geochimica et Cosmochimica Acta* 59:4939–4949.

Mazor E., Heymann D., and Anders E. 1970. Noble gases in carbonaceous chondrites. *Geochimica et Cosmochimica Acta* 34: 781–824.

Mittlefehldt D. W., McCoy T. J., Goodrich C. A., and Kracher A. 1998. Non-chondritic meteorites from asteroidal bodies. In *Planetary materials,* edited by Papike J. J. Washington D.C.: Mineralogical Society of America. *Reviews in Mineralogy* 36:73–93.

Mori H. and Takeda H. 1988. TEM observation of carbonaceous material in the Dyalpur ureilite. Proceedings, 19th Lunar and Planetary Science Conference.

Müller H. W. and Zähringer J. 1969. Rare gases in stony meteorites. In *Meteorite research,* edited by Millman P. M. Dordrecht: D. Reidel. 942 p.

Nagao K., Okazaki R., Sawada S., and Nakamura N. 1999. Noble gases and K-Ar ages of five Rumuruti chondrites Yamato (Y)-75302, Y-791827, Y-793575, Y-82002, and Asuka-881988. *Antarctic Meteorite Research* 12:81–93.

Nakamura T., Nagao K., and Takaoka N. 2000. Microdistribution of heavy primordial noble gases in ureilites. *Meteoritics & Planetary Science* 35:A117.

Nakamuta Y. and Aoki Y. 2000. Mineralogical evidence for the origin of diamond in ureilites. *Meteoritics & Planetary Science* 35:487–493.

Nakamuta Y. and Aoki Y. 2001. Catalytic high-pressure formation of diamond in ureilites. *Meteoritics & Planetary Science* 36:A146.

Nakamuta Y., Aoki Y., and Kojima H. 2002. Classification of ureilites based on characteristics of carbon minerals. *Antarctic Meteorites XXVII*. Papers Presented to the 27th Symposium on Antarctic Meteorites, NIPR, Tokyo, June 11-13, 2002. pp. 117–119.

Nishiizumi K., Regnier S., and Marti K. 1980. Cosmic ray exposure ages of chondrites, pre-irradiation and constancy of cosmic ray flux in the past. *Earth and Planetary Science Letters* 50:156–170.

Ott U., Löhr H. P., and Begemann F. 1984. Ureilites: The case of missing diamonds and a new neon component. *Meteoritics* 19: 287–288.

Ott U., Löhr H. P., and Begemann F. 1985. Trapped noble gases in 5 more ureilites and the possible role of Q. Proceedings, 16th Lunar and Planetary Science Conference. pp. 639–640.

Ott U., Löhr H. P., and Begemann F. 1986. Noble gases in ALH 82130: Comparison with ALHA78019 and diamond-bearing ureilites. *Meteoritics* 21:477–478.

Ott U., Löhr H. P., and Begemann F. 1993. Solar noble gases in

polymict ureilites and an update on ureilite noble gas data. *Meteoritics* 28:415–416.

Ozima M. and Podosek F. A. 2002. *Noble gas geochemistry.* 2nd edition. Cambridge: Cambridge University Press. 286 p.

Rai V. K., Murty S. V. S., and Ott U. 2001. Nitrogen and noble gases in two Antarctic ureilites ALH 81101 and ALH 82130. *Meteoritics & Planetary Science* 36:A171.

Rai V. K., Murty S. V. S., and Ott U. 2002. Nitrogen in diamond-free ureilite Allan Hills 78019: Clues to the origin of diamond in ureilite. *Meteoritics & Planetary Science* 37:1045–1055.

Ringwood A. E. 1960. The Novo Urei meteorite. *Geochimica et Cosmochimica Acta* 20:1–4.

Sato Y., Matsumoto S., Kamo M., and Setaka N. 1984. Vapor deposition of diamond. *Surface Science* 5:54–60.

Takaoka N., Nakashima D., and Nakamura T. 2001. Fractionation and trapping sites of primordial noble gases in ureilites. *Meteoritics & Planetary Science* 36:A203.

Takeda H., Ishii T., Otsuki M., Nakamuta Y., and Nakamura T. 2001. Mineralogy of a new weakly shocked ureilite, Dar al Gani 868 with diamonds. *Meteoritics & Planetary Science* 36:A203–A204.

Urey H. C. 1956. Diamonds, meteorites, and the origin of the solar system. *The Astrophysical Journal* 124:623–637.

Vdovykin G. P. 1970. Ureilites. *Space Science Reviews* 10:483–510.

Wacker J. F. 1986. Noble gases in diamond-free ureilite, ALHA 78019: The roles of shock and nebular processes. *Geochimica et Cosmochimica Acta* 50:633–642.

Wasson J. T., Chou C. L., Bild R. W., and Baedecker P. A. 1976. Classification of and elemental fractionation among ureilites. *Geochimica et Cosmochimica Acta* 40:1449–1458.

Weber H. W., Hintenberger H., and Begemann F. 1971. Noble gases in the Haverö ureilite. *Earth and Planetary Science Letters* 13: 205–209.

Weber H. W., Begemann F., and Hintenberger H. 1976. Primordial gases in graphite-diamond-kamacite inclusions from the Haverö ureilite. *Earth and Planetary Science Letters* 29:81–90.

Wieler R., Anders E., Baur H., Lewis R. S., and Signer P. 1992. Characterisation of Q-gases and other noble gas components in the Murchison meteorite. *Geochimica et Cosmochimica Acta* 56: 2907–2921.

Wilkening L. L. and Marti K. 1976. Rare gases and fossil particle tracks in the Kenna ureilite. *Geochimica et Cosmochimica Acta* 40:1465–1473.

APPENDIX

Table A1. Isotopic ratios and concentrations of noble gases released from ALH 78019 and Kenna by crushing and heating.[a]

	^{4}He	^{3}He/^{4}He	^{22}Ne	^{20}Ne/^{22}Ne	^{21}Ne/^{22}Ne	^{36}Ar	^{38}Ar/^{36}Ar	^{40}Ar/^{36}Ar
ALH 78019								
Crushing AC (0.0871 g)								
AC–1 (300 strokes)	1.76	0.00838 ± 0.00015	0.0345	10.03 ± 0.12	0.0227 ± 0.0051	123	0.18832 ± 0.00035	1.3845 ± 0.0092
AC–2 (300 strokes)	1.45	0.00550 ± 0.00011	0.0115	10.17 ± 0.35	(0.047 ± 0.014)	21.7	0.18816 ± 0.00037	0.707 ± 0.043
AC–3 (300 strokes)	0.891	0.00415 ± 0.00018	0.00625	9.93 ± 0.43	(0.038 ± 0.020)	8.70	0.00039 ± 0.18784	0.15 ± 0.11
AC–4 (300 strokes)	0.712	0.00421 ± 0.00033	0.00339	11.01 ± 0.67	(0.04 ± 0.02)	5.87	0.18802 ± 0.00036	(1.4318 ± 0.0050)
Total	4.81	0.00611	0.0556	10.11	0.023	159	0.1883	1.22
Pyrolysis AP1 (0.0093 g)								
AP1–600 (600ºC)	3.44	(0.0295 ± 0.00011)	0.00295	9.8 ± 1.1	(0.200 ± 0.044)	12.7	0.18754 ± 0.00036	11.43 ± 0.68
AP1–1800 (1800ºC)	175	0.01012 ± 0.00073	1.21	6.904 ± 0.049	0.3101 ± 0.0036	655	0.18627 ± 0.00033	0.609 ± 0.028
AP1–1850 (1850ºC)	(98.0)	(0.00075 ± 0.0001)3	(0.0581)	(6.83 ± 0.47)	(0.134 ± 0.019)	11.2	0.18724 ± 0.00046	(14.537 ± 0.019)
Total	179	0.0101	1.24	6.97	0.310	679	0.1863	0.81
Pyrolysis AP2 (0.0112 g)								
AP2–600 (600ºC)	5.09	(0.00313 ± 0.00016)	0.0336	10.2 ± 1.0	(0.1593 ± 0.0070)	11.7	0.18762 ± 0.00023	28.62 ± 0.53
AP2–1800 (1800ºC)	205	0.01038 ± 0.00061	1.63	7.693 ± 0.057	0.2457 ± 0.0029	776	0.18771 ± 0.00016	0.754 ± 0.020
AP2–1850 (1850ºC)	0.893	(0.000417 ± 0.000062)	(0.0479)	(9.00 ± 0.43)	(0.0728 ± 0.0099)	6.07	0.18745 ± 0.00049	7.5 ± 2.5
Total	211	0.0104	1.66	7.74	0.246	793	0.1877	1.22
Kenna								
Crushing KC (0.0898 g)								
KC–1 (300 strokes)	13.3	0.15890 ± 0.00080	0.218	1.3267 ± 0.0099	0.8290 ± 0.0077	16.7	0.18901 ± 0.00057	1.529 ± 0.063
KC–2 (300 strokes)	10.9	0.1573 ± 0.0030	0.202	1.1367 ± 0.0096	0.8489 ± 0.0042	11.1	0.18859 ± 0.00048	0.791 ± 0.094
KC–3 (300 strokes)	7.3	0.14259 ± 0.00075	0.135	1.060 ± 0.018	0.8529 ± 0.0050	5.71	0.18978 ± 0.00034	0.27 ± 0.18
KC–4 (300 strokes)	5.5	0.1488 ± 0.0017	0.106	1.040 ± 0.029	0.868 ± 0.028	4.26	0.18928 ± 0.00044	(1.9715 ± 0.0070)
KC–5 (600 strokes)	8.0	0.13725 ± 0.00071	0.159	1.056 ± 0.015	0.8574 ± 0.0045	6.24	0.18964 ± 0.00037	0.20 ± 0.17
KC–6 (600 strokes)	6.5	0.13565 ± 0.00076	0.108	0.997 ± 0.016	0.8587 ± 0.0051	4.69	0.18943 ± 0.00044	(1.6678 ± 0.0058)
Total	51.5	0.1489	0.928	1.13	0.850	48.7	0.1892	0.93
Pyrolysis KP1 (0.0236 g)								
KP1–600 (600ºC)	807	0.1913 ± 0.0012	1.99	0.934 ± 0.011	0.8875 ± 0.0027	7.16	0.19408 ± 0.00030	73.30 ± 0.27
KP1–1800 (1800ºC)	3118	0.14513 ± 0.00091	185	0.8684 ± 0.0017	0.87157 ± 0.00066	934	0.19800 ± 0.00014	0.4972 ± 0.0089
KP1–1850 (1850ºC)	2.12	(0.002200 ± 0.000019)	0.0120	5.7 ± 1.3	0.491 ± 0.088	1.58	0.1912 ± 0.0010	10.0 ± 5.1
Total	3927	0.1546	187	0.87	0.872	943	0.1980	1.05
Pyrolysis KP2 (0.0069 g)								
KP2–600 (600ºC)	1334	0.1880 ± 0.0025	3.56	0.881 ± 0.014	0.8827 ± 0.0044	10.2	0.19398 ± 0.00077	112.26 ± 0.77
KP2–1800 (1800ºC)	1852	0.1545 ± 0.0015	154	0.8574 ± 0.0013	0.8782 ± 0.0012	635	0.20116 ± 0.00020	1.359 ± 0.039
KP2–1850 (1850ºC)	2.90	(0.001714 ± 0.000080)	0.108	1.34 ± 0.64	0.877 ± 0.070	9.39	0.18794 ± 0.00057	3.6 ± 2.6
Total	3189	0.1685	157	0.86	0.878	654	0.2010	2.64
Blank Runs								
Crushing								
(500 strokes)	0.00437	0.02630 ± 0.00077	0.000196	4.68 ± 0.47	0.234 ± 0.049	0.00253	0.1911 ± 0.0014	287.94 ± 0.70
600ºC	0.698	0.00041 ± 0.00012	0.000307	5.99 ± 0.40	0.319 ± 0.077	0.00235	0.1909 ± 0.0035	289.8 ± 1.1
1850ºC	1.02	0.000338 ± 0.000058	0.000540	7.32 ± 0.55	0.219 ± 0.033	0.00527	0.1890 ± 0.0018	292.04 ± 0.91

[a]Concentrations are given in 10^{-9} cm^3 STP/g, while amounts of blank gases are in 10^{-9} cm^3 STP. The blank corrections are applied for concentrations and isotopic ratios of every element (numbers in parentheses are not corrected for the blank). Presented errors are 1σ. Uncertainties for concentrations are estimated to be 10%.

Table A2. Isotopic ratios and concentrations of noble gases released from ALH 78019 and Kenna by crushing and heating.[a]

	^{84}Kr	^{78}Kr/^{84}Kr	^{80}Kr/^{84}Kr	^{82}Kr/^{84}Kr	^{83}Kr/^{84}Kr	^{86}Kr/^{84}Kr
ALH 78019						
Crushing AC (0.0871 g)						
AC–1 (300 strokes)	0.652	0.00622 ± 0.00015	0.03972 ± 0.00032	0.20253 ± 0.00074	0.20030 ± 0.00049	0.31041 ± 0.00092
AC–2 (300 strokes)	0.146	0.00617 ± 0.00011	0.03969 ± 0.00048	0.2027 ± 0.0011	0.20362 ± 0.00096	0.3112 ± 0.0016
AC–3 (300 strokes)	0.0412	0.00605 ± 0.00030	0.03971 ± 0.00071	0.2009 ± 0.0028	0.2016 ± 0.0023	0.3110 ± 0.0025
AC–4 (300 strokes)	0.0315	0.00612 ± 0.00020	0.04053 ± 0.00036	0.2043 ± 0.0024	0.2024 ± 0.0026	0.3073 ± 0.0037
Total	0.871	0.00620	0.03974	0.2025	0.2010	0.3104
Pyrolysis AP1 (0.0093 g)						
AP1–600 (600ºC)	0.0907	0.00592 ± 0.00065	0.0414 ± 0.0030	0.212 ± 0.016	0.2085 ± 0.0078	0.3053 ± 0.0092
AP1–1800 (1800ºC)	3.23	0.00596 ± 0.00011	0.03940 ± 0.00036	0.2022 ± 0.0010	0.20408 ± 0.00084	0.3159 ± 0.0015
AP1–1850 (1850ºC)	0.0514	ND[b]	ND	ND	ND	ND
Total	3.38	0.00596	0.03945	0.2025	0.2042	0.3156
Pyrolysis AP2 (0.0112 g)						
AP2–600 (600ºC)	0.179	0.00622 ± 0.00030	0.0396 ± 0.0011	0.2014 ± 0.0019	0.2023 ± 0.0024	0.3093 ± 0.0046
AP2–1800 (1800ºC)	3.77	0.00608 ± 0.00013	0.03955 ± 0.00057	0.2002 ± 0.0018	0.2003 ± 0.0031	0.3095 ± 0.0042
AP2–1850 (1850ºC)	0.0288	ND	ND	ND	ND	ND
Total	3.97	0.00609	0.03955	0.2003	0.2004	0.3095
Kenna						
Crushing KC (0.0898 g)						
KC–1 (300 strokes)	0.283	0.00614 ± 0.00012	0.03985 ± 0.00027	0.20332 ± 0.00077	0.20430 ± 0.00092	0.3140 ± 0.0014
KC–2 (300 strokes)	0.215	0.00621 ± 0.00013	0.03965 ± 0.00034	0.2025 ± 0.0011	0.20289 ± 0.00078	0.3125 ± 0.0014
KC–3 (300 strokes)	0.129	0.00617 ± 0.00014	0.03938 ± 0.00039	0.2020 ± 0.0012	0.2025 ± 0.0012	0.3120 ± 0.0019
KC–4 (300 strokes)	0.080	0.00609 ± 0.00018	0.03964 ± 0.00046	0.2015 ± 0.0011	0.20246 ± 0.00092	0.3099 ± 0.0021
KC–5 (600 strokes)	0.114	0.00603 ± 0.00013	0.03934 ± 0.00039	0.20185 ± 0.00087	0.2019 ± 0.0012	0.3111 ± 0.0011
KC–6 (600 strokes)	0.081	0.00613 ± 0.00022	0.03906 ± 0.00036	0.2015 ± 0.0013	0.20257 ± 0.00076	0.3118 ± 0.0021
Total	0.902	0.00614	0.03958	0.2024	0.2031	0.3124
Pyrolysis KP1 (0.0236 g)						
KP1–600 (600ºC)	0.265	0.00629 ± 0.00029	0.04009 ± 0.00065	0.2030 ± 0.0020	0.2034 ± 0.0026	0.3059 ± 0.0030
KP1–1800 (1800ºC)	6.60	0.00617 ± 0.00014	0.03986 ± 0.00074	0.2032 ± 0.0016	0.2036 ± 0.0018	0.3119 ± 0.0016
KP1–1850 (1850ºC)	0.00992	0.0071 ± 0.0018	0.0396 ± 0.0061	0.208 ± 0.014	0.196 ± 0.016	0.303 ± 0.024
Total	6.88	0.00618	0.03987	0.2032	0.2036	0.3117
Pyrolysis KP2 (0.0059 g)						
KP2–600 (600ºC)	0.863	0.00612 ± 0.00018	0.03908 ± 0.00076	0.2008 ± 0.0015	0.2016 ± 0.0015	0.3090 ± 0.0025
KP2–1800 (1800ºC)	3.84	0.00604 ± 0.00016	0.03966 ± 0.00043	0.20247 ± 0.00091	0.20374 ± 0.00088	0.3137 ± 0.0019
KP2–1850 (1850ºC)	0.0715	ND	ND	ND	ND	ND
Total	4.77	0.00605	0.03955	0.2022	0.2033	0.3129
Blank Runs						
Crushing						
(500 strokes)	0.0000794	0.0079 ± 0.0024	0.0418 ± 0.0037	0.2062 ± 0.0080	0.206 ± 0.021	0.303 ± 0.011
600ºC	0.000127	0.0068 ± 0.0012	0.0398 ± 0.0044	0.2099 ± 0.0099	0.2033 ± 0.0083	0.318 ± 0.012
1850ºC	0.000225	0.00686 ± 0.00095	0.0395 ± 0.0031	0.1991 ± 0.0049	0.1942 ± 0.0063	0.311 ± 0.013

[a]Concentrations are given in 10^{-9} cm^3 STP/g, while amounts of blank gases are in 10^{-9} cm^3 STP. The blank corrections are applied for concentrations and isotopic ratios of every element (numbers in parentheses are not corrected for the blank). Presented errors are 1σ. Uncertainties for concentrations are estimated to be 10%.

[b]ND = not determined.

Table A3. Isotopic ratios and concentrations of noble gases released from ALH 78019 and Kenna by crushing and heating.[a]

	^{132}Xe	^{124}Xe/^{132}Xe	^{126}Xe/^{132}Xe	^{128}Xe/^{132}Xe	^{129}Xe/^{132}Xe	^{130}Xe/^{132}Xe	^{131}Xe/^{132}Xe	^{134}Xe/^{132}Xe	^{136}Xe/^{132}Xe
ALH 78019									
Crushing AC (0.0871 g)									
AC–1 (300 strokes)	0.326	0.004673 ± 0.000085	0.004134 ± 0.000066	0.08423 ± 0.00027	1.0304 ± 0.0017	0.16560 ± 0.00055	0.8198 ± 0.0017	0.38636 ± 0.00091	0.3201 ± 0.0013
AC–2 (300 strokes)	0.0835	0.00451 ± 0.00010	0.00408 ± 0.00020	0.08249 ± 0.00046	1.0293 ± 0.0039	0.16218 ± 0.00073	0.8190 ± 0.0024	0.3806 ± 0.0022	0.3163 ± 0.0019
AC–3 (300 strokes)	0.0253	0.00481 ± 0.00019	0.00425 ± 0.00022	0.0829 ± 0.0013	1.0331 ± 0.0093	0.1622 ± 0.0015	0.8191 ± 0.0047	0.3780 ± 0.0028	0.3153 ± 0.0031
AC–4 (300 strokes)	0.0168	0.00462 ± 0.00023	0.00387 ± 0.00040	0.0826 ± 0.0015	1.0333 ± 0.0060	0.1630 ± 0.0013	0.8177 ± 0.0097	0.3792 ± 0.0057	0.3169 ± 0.0029
Total	0.452	0.00465	0.00412	0.0838	1.030	0.1647	0.8195	0.3846	0.3190
Pyrolysis AP1 (0.0093 g)									
AP1–600 (600ºC)	0.0509	0.00435 ± 0.00057	0.00368 ± 0.00030	0.0806 ± 0.0023	1.026 ± 0.017	0.1609 ± 0.0040	0.814 ± 0.018	0.3767 ± 0.0047	0.3190 ± 0.0071
AP1–1800 (1800ºC)	1.57	0.00461 ± 0.00015	0.004136 ± 0.000088	0.08290 ± 0.00051	1.0315 ± 0.0038	0.16371 ± 0.00071	0.8204 ± 0.0032	0.3818 ± 0.0024	0.3180 ± 0.0027
AP1–1850 (1850ºC)	0.0364	ND[b]	ND	ND	ND	ND	ND	ND	ND
Total	1.65	0.00461	0.00412	0.0828	1.031	0.1636	0.8202	0.3816	0.3181
Pyrolysis AP2 (0.0112 g)									
AP2–600 (600ºC)	0.112	0.00383 ± 0.00050	0.00354 ± 0.00014	0.0745 ± 0.0016	0.9904 ± 0.0094	0.1554 ± 0.0033	0.7991 ± 0.0074	0.3862 ± 0.0035	0.3287 ± 0.0043
AP2–1800 (1800ºC)	1.77	0.004593 ± 0.000074	0.004139 ± 0.000054	0.08292 ± 0.00053	1.0295 ± 0.0029	0.1635 ± 0.0012	0.8178 ± 0.0019	0.3817 ± 0.0017	0.3194 ± 0.0021
AP2–1850 (1850ºC)	0.0224	ND	ND	ND	ND	ND	ND	ND	ND
Total	1.91	0.00455	0.00410	0.0824	1.027	0.1630	0.8167	0.3820	0.3200
Kenna									
Crushing KC (0.0898 g)									
KC–1 (300 strokes)	0.431	0.004722 ± 0.000075	0.004238 ± 0.000096	0.08404 ± 0.00023	1.0330 ± 0.0028	0.16544 ± 0.00079	0.8215 ± 0.0015	0.3840 ± 0.0018	0.3212 ± 0.0015
KC–2 (300 strokes)	0.390	0.004793 ± 0.000041	0.004197 ± 0.000044	0.08455 ± 0.00021	1.0296 ± 0.0023	0.16723 ± 0.00055	0.8206 ± 0.0020	0.38711 ± 0.00076	0.3236 ± 0.0016
KC–3 (300 strokes)	0.249	0.004713 ± 0.000067	0.004173 ± 0.000077	0.08356 ± 0.00034	1.0318 ± 0.0038	0.16422 ± 0.00077	0.8189 ± 0.0012	0.3819 ± 0.0016	0.3215 ± 0.0015
KC–4 (300 strokes)	0.144	0.00461 ± 0.00010	0.00416 ± 0.00073	0.08292 ± 0.00046	1.0302 ± 0.0025	0.1636 ± 0.0011	0.8210 ± 0.0012	0.38281 ± 0.00057	0.3171 ± 0.0021
KC–5 (600 strokes)	0.198	0.004662 ± 0.000053	0.004219 ± 0.000072	0.08325 ± 0.00043	1.0349 ± 0.0023	0.16399 ± 0.00055	0.8190 ± 0.0030	0.38576 ± 0.00057	0.3230 ± 0.0011
KC–6 (600 strokes)	0.141	0.004616 ± 0.000078	0.00423 ± 0.00010	0.08274 ± 0.00054	1.0322 ± 0.0039	0.1636 ± 0.0012	0.82108 ± 0.00201	0.3801 ± 0.0012	0.3176 ± 0.0014
Total	1.55	0.00471	0.00421	0.08377	1.0319	0.1652	0.8205	0.3842	0.3214
Pyrolysis KP1 (0.0236 g)									
KP1–600 (600ºC)	0.139	0.00419 ± 0.00027	0.00373 ± 0.00021	0.0784 ± 0.0011	1.0040 ± 0.0061	0.1588 ± 0.0026	0.8043 ± 0.0053	0.3842 ± 0.0099	0.3232 ± 0.0061
KP1–1800 (1800ºC)	8.05	0.004403 ± 0.000091	0.004004 ± 0.000046	0.08152 ± 0.00046	1.0173 ± 0.0038	0.16249 ± 0.00058	0.8177 ± 0.0021	0.3864 ± 0.0017	0.3248 ± 0.0017
KP1–1850 (1850ºC)	0.00819	0.0038 ± 0.0016	0.00372 ± 0.00088	0.0811 ± 0.0035	1.070 ± 0.039	0.1560 ± 0.0076	0.815 ± 0.027	0.386 ± 0.015	0.335 ± 0.015
Total	8.20	0.00440	0.00400	0.0815	1.0171	0.1624	0.8174	0.3863	0.3248
Pyrolysis KP2 (0.0069 g)									
KP2–600 (600ºC)	0.686	0.00369 ± 0.00011	0.00340 ± 0.00015	0.0728 ± 0.0010	0.9838 ± 0.0058	0.1517 ± 0.0014	0.7902 ± 0.0043	0.3873 ± 0.0019	0.3295 ± 0.0013
KP2–1800 (1800ºC)	3.02	0.004494 ± 0.00009	0.004135 ± 0.000087	0.08275 ± 0.00051	1.0278 ± 0.0056	0.16372 ± 0.00073	0.8203 ± 0.0021	0.38385 ± 0.00097	0.3208 ± 0.0013
KP2–1850 (1850ºC)	0.0759	ND	ND	ND	ND	ND	ND	ND	ND
Total	3.79	0.00434	0.00400	0.0809	1.0197	0.1615	0.8147	0.3845	0.3224
Blank Runs									
Crushing (500 strokes)	0.0000401	0.0175 ± 0.0038	0.0039 ± 0.0021	0.0681 ± 0.0059	1.126 ± 0.060	0.162 ± 0.011	0.802 ± 0.030	0.385 ± 0.013	0.326 ± 0.026
600ºC	0.0000248	0.0199 ± 0.0046	0.0055 ± 0.0014	0.0737 ± 0.0089	1.248 ± 0.021	0.163 ± 0.019	0.796 ± 0.035	0.395 ± 0.030	0.338 ± 0.031
1850ºC	0.0000343	0.0218 ± 0.0052	0.0052 ± 0.0015	0.0734 ± 0.0077	1.196 ± 0.072	0.155 ± 0.018	0.803 ± 0.062	0.385 ± 0.017	0.351 ± 0.032

[a]Concentrations are given in 10^{-9} cm^3 STP/g, while amounts of blank gases are in 10^{-9} cm^3 STP. The blank corrections are applied for concentrations and isotopic ratios of every element (numbers in parentheses are not corrected for the blank). Presented errors are 1σ. Uncertainties for concentrations are estimated to be 10%.

[b]ND = not determined.